International Journal of Engineering Research & Technology (IJERT)
ISSN: 2278-0181
Vol. 4 Issue 12, December-2015

The Multi-constellation Single Epoch GNSS Attitude Determination based on Orthogonal Transformation Approach

Wantong Chen
School of Electronics and Information Engineering
Civil Aviation University of China
Tianjin, China

Abstract*—Real-time dynamic attitude determination using GNSS signal is of great significance for the vehicles. The single epoch attitude determination algorithm utilizing multi-frequency multi-mode observation is the point for the current research, since it is insensitive to cycle slips and has a higher success rate and a higher accuracy than that of attitude determination with single frequency observation. The coverage, integrity and availability can also be improved for the practical application. In this contribution, the GNSS baseline model which combining multiple constellations is discussed based on orthogonal transformation of single differences, which is a numerically stable approach; the computation process of float solution for the GNSS model is deduced and the assessment of accuracy is achieved for GNSS compass based on the actual L1/L2/B1 data. The experiment demonstrates that the accuracy of heading can reach 0.1 degree/meter and the accuracy of elevation can reach 0.2 degree/meter for L1/L2/B1 triple-frequency observation and it *is two times higher than that of the B1 single frequency observation.

Keywords—GNSS; attitude determination; orthogonal transformation; integer ambiguity resolution; accuracy

I. Introduction

The high precision, real-time attitude determination system is indispensable and important for many different dynamic vehicles in terrestrial, sea, air and space, because it takes an important place in the development of many navigation, guidance and control systems. The attitude determination is in essence the problem of estimating the precise orientation of a platform which carries the sensors with respect to a chosen frame of reference. It is described normally by attitude coordinates, and consists of at least two coordinates for compass type attitude determination (heading angle and pitch angle). Many sensors and technologies are available to estimate the attitude of a platform, such as the magnetic compass and the gyrocompass. In recent years, there is a growing interest in GNSS compass type attitude determination and GNSS-based full attitude determination. Compared with the above two devices, the GNSS compass can point to any desired direction and it presents several obvious advantages: it is low-cost and less drift, minor maintenance is required and there is no ground reference [1]. For this technique, two antennas are attached to a vehicle, and then a baseline vector defined as a vector from reference antenna to another antenna can be determined using GNSS relative positioning technique. Thus, one is able to estimate the pointing direction, namely the compass solution, with two antennae/single baseline, while configuration of three or more non-collinear antennae allow the user to estimate the full attitude of a platform (heading/yaw, elevation/pitch and roll).

In order to obtain accurate measurements of a platform attitude, the GNSS carrier phase observations must be employed. However, the carrier phase observations are inherently affected by an integer ambiguity, and once this has been done successfully, the carrier phase data will act as very precise pseudorange data, thus making very precise attitude determination possible [2]. Integer ambiguity resolution (IAR) is the process of resolving the unknown cycle ambiguities of the carrier phase data as integer, and many studies have been carried out to investigate the IAR method and performance of GNSS-based attitude determination. More recent attitude determination methods make use of the Constrained LAMBDA method to estimate the integer ambiguity, which is a fast, reliable and widely used implementation of the ILS (Integer Least-Squares) estimator [3]. To utilize this method, the float ambiguity solution must be estimated based on GNSS carrier phase/code double difference (DD) observation equations. However, specific care must be taken in parametrizing the phase ambiguities when there are cycle slips [4], which is one challenging case of GNSS data processing. Ambiguity resolution in single epoch can guarantee a total independence from carrier phase slips and losses of lock, as this technique uses only the fractional value of carrier phase measurement. Thus, the focus moves on the single epoch ambiguity resolution for GNSS-base attitude determination.

The probability of correct integer ambiguity estimation, the so-called ambiguity success rate, is determined by the strength of the underlying GNSS model; the stronger the model, the higher the success rate. Since the success rate of single frequency ambiguity resolution is often not high enough for single epoch, the multi-frequency scheme is focused for strengthening the model and improving the success rate [5]. Beside the success rate and the accuracy, the coverage, integrity and availability also take an important place in the practical application of GNSS compass. This can be resolved by using observables from multiple GNSS constellations. Nowadays, several different implementations of GNSS including GPS of the USA, Glonass from Russia, Galileo from European Union, and Compass from China as well as regional navigation constellations such as QZSS of

This work is supported by the Scientific Research Fund of Civil Aviation University of China (Grant No.2013QD27X).

Japan and IRNSS of India are and will be available for users. It is desired from the perspective of users to exploit the possibilities and opportunities of fusing signals from different constellations so as to enhance coverage, accuracy, integrity, and availability. In this contribution, the multi-frequency multi-constellation GNSS compass model is studied, based on the orthogonal transformation of single difference equations. The assessment of accuracy is also achieved for this scheme. Actual experiments based on L1/L2/B1 observations have been performed to verify the correctness of new method and the accuracy of attitude determination.

II. THE GNSS COMPASS MODEL

A. Heading and Elevation Estimation

For the GNSS compass system, two antennas are utilized to provide the observability of heading (or yaw) and elevation (or pitch). If the baseline vector from reference antenna to another antenna is parameterized with respect to the local East-North-Up frame, the heading ψ and the elevation θ can be computed from the baseline components (coordinates) b_E, b_N and b_U as

$$\psi = \tan^{-1}\left(\frac{b_E}{b_N}\right), \theta = \tan^{-1}\left(\frac{b_U}{\sqrt{b_N^2 + b_E^2}}\right) \quad (1)$$

B. GNSS Baseline Model

For single baseline, the standard GNSS model is given by the linear observation equations, which is called a (mixed) integer least-squares (ILS) problem [6]. It is defined as:

$$E(\boldsymbol{y}) = \boldsymbol{Aa} + \boldsymbol{Bx}, D(\boldsymbol{y}) = \boldsymbol{Q}_y, \boldsymbol{a} \in Z^n, \boldsymbol{x} \in R^p \quad (2)$$

where $\boldsymbol{y}$ is the given GNSS data vector, and $\boldsymbol{a}$ and $\boldsymbol{x}$ are the unknown parameter vectors of order n and p respectively. E(·) and D(·) denote the expectation and dispersion operators, respectively, and $\boldsymbol{A}$ and $\boldsymbol{B}$ are the given design matrices that link the data vector to the unknown parameters. The variance matrix of $\boldsymbol{y}$ is given by the positive definite matrix $\boldsymbol{Q}_y$. The n-vector $\boldsymbol{a}$ contains the integer ambiguities and the real-valued p-vector $\boldsymbol{x}$ contains baseline vector $\boldsymbol{b}$ and other remaining unknown parameters $\boldsymbol{r}$, such as for instance possibly atmospheric delay parameters (troposphere, ionosphere) and clock bias parameter, which depend on the baseline length and difference model respectively.

C. GNSS Compass Model

For the compass problem, the possibly atmospheric delay parameters can omitted due to the very short distance between the two antennas. If the clock bias term is also eliminated with some approach in the model, then the real-valued p-vector $\boldsymbol{x}$ only contains baseline vector $\boldsymbol{b}$. Since the baseline length is often known in practical applications, this priori given baseline information can be treated as a useful constraint as well. Thus, in this case the standard GNSS model (2) is extended to

$$\begin{aligned} &E(\boldsymbol{y}) = \boldsymbol{Aa} + \boldsymbol{Bb}, \boldsymbol{a} \in Z^n, \boldsymbol{b} \in R^3, \|\boldsymbol{b}\| = l \\ &D(\boldsymbol{y}) = \boldsymbol{Q}_y \end{aligned} \quad (3)$$

This nonlinearly constrained model will be referred to as the GNSS Compass model. It is a linear GNSS model with a nonlinear constraint on the baseline vector [3]. Once $\boldsymbol{a}$ is resolved, the least-squares solution for $\boldsymbol{b}$, can be written as

$$\hat{\boldsymbol{b}}(\boldsymbol{a}) = \left(\boldsymbol{B}^T \boldsymbol{Q}_y^{-1} \boldsymbol{B}\right)^{-1} \boldsymbol{B}^T \boldsymbol{Q}_y^{-1} (\boldsymbol{y} - \boldsymbol{Aa}) \quad (4)$$

The variance-covariance matrix of conditional least-squares solution of $\boldsymbol{b}$ is given as

$$\boldsymbol{Q}_{\hat{b}(\boldsymbol{a})} = \left(\boldsymbol{B}^T \boldsymbol{Q}_y^{-1} \boldsymbol{B}\right)^{-1} \quad (5)$$

Now we consider the case that $\boldsymbol{a}$ is completely unknown. To solve the GNSS model (3), one usually applies the least-squares principle. This amounts to solving the following minimization problem:

$$\begin{aligned} &\min_{\boldsymbol{a} \in Z^n, \boldsymbol{b} \in R^3, \|\boldsymbol{b}\| = l} \|\boldsymbol{y} - \boldsymbol{Aa} - \boldsymbol{Bb}\|_{Q_y}^2 \\ &= \|\hat{\boldsymbol{e}}\|_{Q_y}^2 + \min_{\boldsymbol{a} \in Z^n} \left(\|\hat{\boldsymbol{a}} - \boldsymbol{a}\|_{Q_{\hat{a}}}^2 + \min_{\boldsymbol{b} \in R^3, \|\boldsymbol{b}\| = l} \|\hat{\boldsymbol{b}}(\boldsymbol{a}) - \boldsymbol{b}\|_{Q_{\hat{b}(a)}}^2 \right) \end{aligned} \quad (6)$$

where $\|(\cdot)\|_{Q_y}^2 = (\cdot)^T \boldsymbol{Q}_y^{-1} (\cdot)$ and $\hat{\boldsymbol{e}}$ is the least squares residuals. Note that the minimization problem thus involves two types of constraints: the integer constraints on the ambiguities and the length constraint on the baseline vector. Thus, the integer least-squares principle with quadratic equality constraints is used to formulate the following cost function [7]:

$$\min_{\boldsymbol{a} \in Z^n} \left(\|\hat{\boldsymbol{a}} - \boldsymbol{a}\|_{Q_{\hat{a}}}^2 + \min_{\boldsymbol{b} \in R^3, \|\boldsymbol{b}\| = l} \|\hat{\boldsymbol{b}}(\boldsymbol{a}) - \boldsymbol{b}\|_{Q_{\hat{b}(a)}}^2 \right) \quad (7)$$

In this case, the conditional least-squares solution for $\boldsymbol{b}$ and its variance-covariance matrix are both required for the estimator. The solution to the minimization problem follows therefore as

$$\begin{aligned} &\breve{\boldsymbol{a}} = arg \min_{\boldsymbol{a} \in Z^n} \left(\|\hat{\boldsymbol{a}} - \boldsymbol{a}\|_{Q_{\hat{a}}}^2 + \min_{\boldsymbol{b} \in R^3, \|\boldsymbol{b}\| = l} \|\hat{\boldsymbol{b}}(\boldsymbol{a}) - \boldsymbol{b}\|_{Q_{\hat{b}(a)}}^2 \right) \\ &\breve{\boldsymbol{b}} = \hat{\boldsymbol{b}}(\breve{\boldsymbol{a}}) \end{aligned} \quad (8)$$

This can be solved by the Constrained (C-) LAMBDA method with high efficiency and high success rate [8].

III. MODEL REALIZATION

The short baseline model is often constructed by the double difference method. The paper attempts to address an orthogonal transformation method to construct the short baseline model, solving GNSS compass problem when measurements from multiple constellations are used. The proposed method is seen to be both efficient and accurate.

Firstly, the single-differenced model for single frequency is given, then we deduce the orthogonal transformation model. Next, the multi-frequency single constellation model is created based on the orthogonal transformation model. Finally, the multiple constellation model are presented, which is a combination of multiple multi-frequency single-constellation models.

A. The Single Difference Model for Single Frequency

For two nearby antennas A and B, the Single-Differenced (SD) carrier phase and code observation equations on band L_i of GNSS constellation g can be modeled as

$$\begin{aligned}\lambda_i^g\left(\phi_{i,AB}^{g,k}+a_{i,AB}^{g,k}\right)&=r_{AB}^{g,k}+c\left(\delta t_A-\delta t_B\right)+v_{i,AB}^{g,k}\\ \rho_{i,AB}^{g,k}&=r_{AB}^{g,k}+c\left(\delta t_A-\delta t_B\right)+\mu_{i,AB}^{g,k}\end{aligned} \tag{9}$$

where λ_i^g is the wavelength of L_i carrier; $\phi_{i,AB}^{g,k}$ and $a_{i,AB}^{g,k}$ denote the SD fractional phase and integer ambiguity respectively; $\rho_{i,AB}^{g,k}$ denotes the SD code observable; $v_{i,AB}^{g,k}$ and $\mu_{i,AB}^{g,k}$ denote the SD phase and code observable noise respectively; $r_{AB}^{g,k}$ is the SD geometric range of two receivers for satellite k GNSS constellation g; δt_A and δt_B are clock biases of receiver A and B; c is the velocity of light. For short baseline, since both antennas 'see' the same satellite in the same direction and the lines of sight (LOS) are approximately parallel for both antennas, the SD geometric range of two antennas for satellite k can be treated as the projection of the baseline in the direction of LOS, say $r_{AB}^{g,k}=\boldsymbol{s}^{g,k}\cdot\boldsymbol{b}$ where $\boldsymbol{s}^{g,k}=\left(s_1^{g,k}\quad s_2^{g,k}\quad s_3^{g,k}\right)^T$ is the normalized line-of-sight vector. For m_g visible satellites of stand-alone GNSS constellation g, with $\sigma_{g,i,\phi}^2$ and $\sigma_{g,i,\rho}^2$ being the variance of carrier phase and code on band L_i, the SD carrier phase and code equations can be expressed in compact vector and matrix notation as [9]

$$\begin{aligned}\boldsymbol{y}_{i,S}^{g,\phi}&=\frac{1}{\lambda_i^g}\boldsymbol{E}^g\cdot\boldsymbol{b}-\boldsymbol{a}_{i,S}^g+\frac{1}{\lambda_i^g}\boldsymbol{e}_{m_g}\tau+\boldsymbol{v}_{i,S}^{g,\phi},\ \boldsymbol{v}_{i,S}^{g,\phi}\sim N\left(\boldsymbol{0},2\sigma_{g,i,\phi}^2\boldsymbol{I}_{m_g}\right)\\ \boldsymbol{y}_{i,S}^{g,\rho}&=\frac{1}{\lambda_i^g}\boldsymbol{E}^g\cdot\boldsymbol{b}+\frac{1}{\lambda_i^g}\boldsymbol{e}_{m_g}\tau+\boldsymbol{v}_{i,S}^{g,\rho},\ \boldsymbol{v}_{i,S}^{g,\rho}\sim N\left(\boldsymbol{0},2\sigma_{g,i,\rho}^2\boldsymbol{I}_{m_g}\right)\end{aligned} \tag{10}$$

where $\boldsymbol{y}_{i,S}^{g,\phi}$ and $\boldsymbol{y}_{i,S}^{g,\rho}$ are SD phase and code observations in units of cycles, $\boldsymbol{E}^g$ is the $(m-1)\times 3$ matrix of normalized SD line-of-sight vectors, $\boldsymbol{v}_{i,S}^{g,\phi}$ and $\boldsymbol{v}_{i,S}^{g,\rho}$ are SD phase and code noise vectors, $\boldsymbol{a}_{i,S}^g$ is the SD integer ambiguity vector, $\boldsymbol{e}_{m_g}$ is a vector of order m_g for which each entry is 1 and $\tau=c\left(\delta t_A-\delta t_B\right)$ is the clock bias. All the involved vectors are given as follows:

$$\boldsymbol{y}_{i,S}^{g,\phi}=\begin{bmatrix}\phi_{i,AB}^{g,1}\\ \phi_{i,AB}^{g,2}\\ \vdots\\ \phi_{i,AB}^{g,m}\end{bmatrix},\boldsymbol{y}_{i,S}^{g,\rho}=\begin{bmatrix}\rho_{i,AB}^{g,1}\\ \rho_{i,AB}^{g,2}\\ \vdots\\ \rho_{i,AB}^{g,m_g}\end{bmatrix},\boldsymbol{a}_{i,S}^{g}=\frac{1}{\lambda_i^g}\begin{bmatrix}a_{i,AB}^{g,1}\\ a_{i,AB}^{g,2}\\ \vdots\\ a_{i,AB}^{g,m_g}\end{bmatrix},\boldsymbol{v}_{i,S}^{g,\phi}=\begin{bmatrix}v_{i,AB}^{g,1}\\ v_{i,AB}^{g,2}\\ \vdots\\ v_{i,AB}^{g,m_g}\end{bmatrix},$$
$$\boldsymbol{v}_{i,S}^{g,\rho}=\begin{bmatrix}\mu_{i,AB}^{g,1}\\ \mu_{i,AB}^{g,2}\\ \vdots\\ \mu_{i,AB}^{g,m_g}\end{bmatrix},\boldsymbol{E}^g=\begin{bmatrix}\left(\boldsymbol{s}^{g,1}\right)^T\\ \left(\boldsymbol{s}^{g,2}\right)^T\\ \vdots\\ \left(\boldsymbol{s}^{g,m_g}\right)^T\end{bmatrix},\boldsymbol{e}_{m_g}=\begin{bmatrix}1\\ 1\\ \vdots\\ 1\end{bmatrix}_{m_g\times 1} \tag{11}$$

B. The Orthogonal Transformation Model

The orthogonal transformation of single differences can also eliminate the clock bias term of (10) and the vector of DD integer ambiguities is still available [10]. Let $\boldsymbol{P}^g\in R^{m_g\times m_g}$ be an orthogonal transformation such that $\boldsymbol{P}\boldsymbol{e}_{m_g}=\sqrt{m_g}\boldsymbol{u}_1$ and the Householder transformation is used to form $\boldsymbol{P}^g$ as follows:

$$\boldsymbol{P}^g=\boldsymbol{I}_{m_g}-\frac{2\boldsymbol{t}\boldsymbol{t}^T}{\boldsymbol{t}^T\boldsymbol{t}},\boldsymbol{t}\equiv\boldsymbol{u}_1-\frac{1}{\sqrt{m_g}}\boldsymbol{e}_{m_g} \tag{12}$$

where $\boldsymbol{u}_1=\left(1,0,\cdots,0\right)^T=\left(1\quad \boldsymbol{0}\right)^T$. By simple algebraic operations, we obtain for this matrix

$$\boldsymbol{P}^g=\left[\begin{array}{c|c}\frac{1}{\sqrt{m_g}} & \frac{\boldsymbol{e}_{m_g-1}^T}{\sqrt{m_g}}\\ \hline \frac{\boldsymbol{e}_{m_g-1}}{\sqrt{m_g}} & \boldsymbol{I}_{m_g-1}-\frac{\boldsymbol{e}_{m_g-1}\cdot\boldsymbol{e}_{m_g-1}^T}{m_g-\sqrt{m_g}}\end{array}\right]\equiv\begin{bmatrix}\boldsymbol{p}^g\\ \bar{\boldsymbol{P}}^g\end{bmatrix} \tag{13}$$

where $\bar{\boldsymbol{P}}^g=\begin{bmatrix}\frac{\boldsymbol{e}_{m_g-1}}{\sqrt{m_g}} & \boldsymbol{I}_{m_g-1}-\frac{\boldsymbol{e}_{m_g-1}\cdot\boldsymbol{e}_{m_g-1}^T}{m_g-\sqrt{m_g}}\end{bmatrix}$. Applying $\boldsymbol{P}^g$ to the carrier phase observation of (10), we obtain

$$\begin{bmatrix}\boldsymbol{p}^g\boldsymbol{y}_{i,S}^{g,\phi}\\ \bar{\boldsymbol{P}}^g\boldsymbol{y}_{i,S}^{g,\phi}\end{bmatrix}=\frac{1}{\lambda_i^g}\begin{bmatrix}\boldsymbol{p}^g\boldsymbol{E}^g\\ \bar{\boldsymbol{P}}^g\boldsymbol{E}^g\end{bmatrix}\boldsymbol{b}-\begin{bmatrix}\boldsymbol{p}^g\boldsymbol{a}_{i,S}^g\\ \bar{\boldsymbol{P}}^g\boldsymbol{a}_{i,S}^g\end{bmatrix}+\begin{bmatrix}1\\ \boldsymbol{0}\end{bmatrix}\sqrt{m_g}\beta+\begin{bmatrix}\boldsymbol{p}^g\boldsymbol{v}_{i,S}^{g,\phi}\\ \bar{\boldsymbol{P}}^g\boldsymbol{v}_{i,S}^{g,\phi}\end{bmatrix} \tag{14}$$

Note that only the first equation involves the clock bias term, the remaining part can be written as

$$\bar{\boldsymbol{P}}^g\boldsymbol{y}_{i,S}^{g,\phi}=\frac{1}{\lambda_i^g}\bar{\boldsymbol{P}}^g\boldsymbol{E}^g\boldsymbol{b}-\bar{\boldsymbol{P}}^g\boldsymbol{a}_{i,S}^g+\bar{\boldsymbol{P}}^g\boldsymbol{v}_{i,S}^{g,\phi} \tag{15}$$

It can be verified that [11]

$$\bar{\boldsymbol{P}}^g=\boldsymbol{F}^g\boldsymbol{D}^g,\boldsymbol{F}^g\equiv\boldsymbol{I}_{m_g-1}-\frac{\boldsymbol{e}_{m_g-1}\boldsymbol{e}_{m_g-1}^T}{m_g-\sqrt{m_g}},\boldsymbol{D}^g\equiv\begin{bmatrix}-\boldsymbol{e}_{m_g-1} & \boldsymbol{I}_{m_g-1}\end{bmatrix} \tag{16}$$

where $\boldsymbol{F}^g$ is nonsingular and $\boldsymbol{D}^g$ is the DD operator. Thus, the DD integer ambiguity vector can also be obtained by the following algebraic operations:

$$\bar{\boldsymbol{P}}^g\boldsymbol{a}_{i,S}^g=\boldsymbol{F}^g\boldsymbol{D}^g\boldsymbol{a}_{i,S}^g=\boldsymbol{F}^g\boldsymbol{a}_{i,D}^g \tag{17}$$

Replacing $\bar{\boldsymbol{P}}^g\boldsymbol{a}_{i,S}^g$ in (15) by (17), we obtain

$$\begin{aligned}\bar{\boldsymbol{P}}^g\boldsymbol{y}_{i,S}^{g,\phi}&=\frac{1}{\lambda_i^g}\bar{\boldsymbol{P}}^g\boldsymbol{E}^g\boldsymbol{b}-\boldsymbol{F}^g\boldsymbol{a}_{i,D}^g+\bar{\boldsymbol{P}}^g\boldsymbol{v}_{i,S}^{g,\phi}\\ \bar{\boldsymbol{P}}\boldsymbol{v}_{i,S}^{\phi}&\sim N\left(\boldsymbol{0},2\sigma_{g,i,\phi}^2\boldsymbol{I}_{m_g-1}\right)\end{aligned} \tag{18}$$

where the DD integer ambiguity vector exists. The transformed noise vector still follows the same distribution because orthogonal transformation will not change the statistical properties of white noise. Similarly, applying $\boldsymbol{P}^g$ to the code observation of (10), we obtain the following orthogonal transformation of SD code observation equation:

$$\begin{aligned}\bar{\boldsymbol{P}}^g\boldsymbol{y}_{i,S}^{g,\rho}&=\frac{1}{\lambda_i^g}\bar{\boldsymbol{P}}^g\boldsymbol{E}^g\boldsymbol{b}+\bar{\boldsymbol{P}}^g\boldsymbol{v}_{i,S}^{g,\rho}\\ \bar{\boldsymbol{P}}^g\boldsymbol{v}_{i,S}^{g,\phi}&\sim N\left(\boldsymbol{0},2\sigma_{g,i,\rho}^2\boldsymbol{I}_{m_g-1}\right)\end{aligned} \tag{19}$$

The combination expression of (18) and (19) reads

$$\begin{bmatrix}\boldsymbol{y}_i^{g,\phi}\\ \boldsymbol{y}_i^{g,\rho}\end{bmatrix}=\begin{bmatrix}\boldsymbol{H}_i^g\\ \boldsymbol{H}_i^g\end{bmatrix}\boldsymbol{b}+\begin{bmatrix}-\boldsymbol{F}\\ \boldsymbol{0}\end{bmatrix}\boldsymbol{a}_i^g+\begin{bmatrix}\boldsymbol{v}_i^{g,\phi}\\ \boldsymbol{v}_i^{g,\rho}\end{bmatrix} \tag{20}$$

where $y_i^{g,\phi} = \bar{P}^g y_{i,S}^{g,\phi}$, $y_i^{g,\rho} = \bar{P}^g y_{i,S}^{g,\rho}$, $H_i^g = \frac{1}{\lambda_i^g}\bar{P}^g E^g$,

$a_i^g = D^g a_{i,S}^g, v_i^{g,\phi} = \bar{P}^g v_{i,S}^{g,\phi}, v_i^{g,\rho} = \bar{P}^g v_{i,S}^{g,\rho}$. Thus the standard GNSS model can be obtained as follows:

$$E\left(y_i^g\right) = A_0^g a_i^g + B_i^g b, D\left(y_i^g\right) = Q_{y_i^g}, a_i^g \in Z^{m_g-1}, b \in R^3 \quad (21)$$

where all the terms are given as

$$y_i^g = \begin{bmatrix} y_i^{g,\phi} \\ y_i^{g,\rho} \end{bmatrix}, A_0^g = \begin{bmatrix} -F_{m_g} \\ 0 \end{bmatrix}, B_i^g = \frac{1}{\lambda_i^g}\bar{P}^g G^g,$$
$$G^g = e_2 \otimes E^g, Q_{y_i^g} = \begin{bmatrix} 2\sigma_{g,i,\phi}^2 I_{m_g-1} & \\ & 2\sigma_{g,i,\rho}^2 I_{m_g-1} \end{bmatrix} \quad (22)$$

C. The Multi-frequency Single-constellation Model

Assume that the number of available frequencies is *Ig* for the GNSS constellation *g*, the multi-frequency single constellation model can be obtained on basis of the combinations of (21):

$$E\left(y^g\right) = A^g a^g + B^g b, D\left(y^g\right) = Q_{y^g}$$
$$a^g \in Z^{(m_g-1)\times I_g}, b \in R^3 \quad (23)$$

where

$$y^g = \underset{i=1,\cdots I_g}{col}\left\{y_i^g\right\}, a^g = \underset{i=1,\cdots I_g}{col}\left\{a_i^g\right\}, A^g = I_{I_g} \otimes A_0^g,$$
$$B^g = \underset{i=1,\cdots I_g}{col}\left\{B_i^g\right\}, Q_{y^g} = \underset{i=1,\cdots I_g}{diag}\left\{Q_{y_i^g}\right\} \quad (24)$$

The notations '*col*' and '*diag*' above are defined as

$$\underset{i=1,\cdots I}{col}\left\{\Lambda_i\right\} = \begin{bmatrix} \Lambda_1 \\ \Lambda_2 \\ \vdots \\ \Lambda_I \end{bmatrix}, \quad \underset{i=1,\cdots I}{diag}\left\{\Lambda_i\right\} = \begin{bmatrix} \Lambda_1 & & & \\ & \Lambda_2 & & \\ & & \ddots & \\ & & & \Lambda_I \end{bmatrix} \quad (25)$$

D. The Multiple Constellations Model

Assume that the number of available constellations is *G*, the multi-frequency single constellation compass model can be written as follows:

$$E(y) = Aa + Bb, D(y) = Q_y, a \in Z^n, b \in R^3, \|b\| = l \quad (26)$$

where

$$y = \underset{g=1,\cdots G}{col}\left\{y^g\right\}, a = \underset{g=1,\cdots G}{col}\left\{a^g\right\}, n = \sum_{g=1}^{G}\left(m_g - 1\right)\times I_g$$
$$A = \underset{g=1,\cdots G}{diag}\left\{A^g\right\}, B = \underset{g=1,\cdots G}{col}\left\{B^g\right\}, Q_y = \underset{g=1,\cdots G}{diag}\left\{Q^g\right\} \quad (27)$$

Now we obtain the multiple constellations GNSS baseline model for single epoch observation, and the expression is consistent with (3).

E. Computation process of float solution for the GNSS model

The solution to (26) can be obtained by resolving cost function (8). However, the float solution must be calculated before the ambiguity search. To gain a clearer computation process and the structure of float solution, it is helpful to first apply the following matrix notations for (26):

$$X_1 = A^T Q_y^{-1} A, X_2 = A^T Q_y^{-1} B, X_3 = B^T Q_y^{-1} B \quad (28)$$

$$l_1 = A^T Q_y^{-1} y, l_2 = B^T Q_y^{-1} y \quad (29)$$

Thus, on basis of (4) and (5), we have

$$Q_{\hat{b}(a)} = X_3^{-1}$$
$$\hat{b}(a) = Q_{\hat{b}(a)}\left(l_2 - X_2^T a\right) \quad (30)$$

With the well-known partition matrix inversion Lemma, the float ambiguity vector and its variance-covariance matrix can be calculated as

$$Q_{\hat{a}} = \left(X_1 - X_2 \cdot Q_{\hat{b}(a)} \cdot X_2^T\right)^{-1}$$
$$\hat{a} = Q_{\hat{a}} \cdot \left(l_1 - X_2 \cdot Q_{\hat{b}(a)} \cdot l_2\right) \quad (31)$$

For the multi-frequency single constellation case, the computation of (28) and (29) has a more direct way, which is given as follows:

$$X_1^g = \underset{i=1,\cdots I_g}{diag}\left\{\frac{1}{2\sigma_{g,i,\phi}^2}\right\}\otimes \Pi_1^g, X_2^g = \underset{i=1,\cdots I_g}{col}\left\{-\frac{1}{2\lambda_i^g \sigma_{g,i,\phi}^2}\right\}\otimes\left(\Pi_2^g E^g\right)$$
$$X_3^g = \omega^g\left(E^g\right)^T \Pi_3^{g,M} E^g, l_1^g = \underset{i=1,\cdots I_g}{col}\left\{-\frac{1}{2\sigma_{g,i,\phi}^2}\Pi_2^g y_{i,S}^{g,\phi}\right\} \quad (32)$$
$$l_2^g = \sum_{i=1}^{I_g}\left(\frac{1}{\lambda_i^g}\left(E^g\right)^T \Pi_3^g\left(\frac{1}{2\sigma_{g,i,\phi}^2}y_{i,S}^{g,\phi} + \frac{1}{2\sigma_{g,i,\rho}^2}y_{i,S}^{g,\rho}\right)\right)$$

where

$$\omega^g = \sum_{i=1}^{I_g}\omega_i^g, \omega_i^g = \left(\frac{1}{2\sigma_{g,i,\phi}^2} + \frac{1}{2\sigma_{g,i,\rho}^2}\right)\frac{1}{\left(\lambda_i^g\right)^2}$$
$$\Pi_1^g = I_{m_g-1} - \frac{1}{m_g}e_{m_g-1}e_{m_g-1}^T, \Pi_3^g = I_{m_g} - \frac{1}{m_g}e_{m_g}e_{m_g}^T \quad (33)$$
$$\Pi_2^g = \begin{bmatrix} -\frac{1}{m_g}e_{m_g-1} & I_{m_g-1} - \frac{1}{m_g}e_{m_g-1}e_{m_g-1}^T \end{bmatrix}$$

F. The Difference of Different Constellations

Both receivers can receive and process signals from different constellations to establish more accurate attitude determination. However, different navigation constellations may differ in their reference frames and time systems. The difference in reference frame is, in general, insignificant and can be easily corrected. On the other hand, since each constellation maintains its time system independently, when the user attempts to process measurements from different constellations, the clock bias with respect to each constellation must be estimated. A possible remedy to account for the timing offset between two constellations is to disseminate the timing offset via both constellations so that the receiver can process measurements from different constellations more coherently [12].

IV. EXPERIMENTS

This section presents the evaluation of the propose method based on actual tests. The accuracies of yaw and pitch are also compared between the multiple constellation scheme and single frequency scheme.

A. Platform and Test Environment

In order to achieve the attitude determination with actual multiple constellation GNSS signals, the NovAtel's OEM628 board is utilized, which is designed with 120 channel and can tracks all current and upcoming GNSS constellations and satellite signals including GPS, GLONASS, Galileo and Compass. Configurable channels optimize satellite availability in any condition, no matter how challenging. For this experiment, the GPS L1/L2 and Compass (or BDS) B1 are exploited to construct the propose model.

Two Trimble® Zephyr™ Model 2 antennas are utilized for the experiment, which contain advanced technology for minimizing multipath, outstanding low elevation satellite tracking, and extremely precise phase center accuracy. Trimble® Zephyr™ Model 2 antenna supports the GPS L1/L2 and Compass (or BDS) B1 bands and has an excellent performance for GNSS relative positioning.

Fig.1 The experiment environment

The experiment was achieved in the playground of Civil Aviation University of China and the baseline was placed in the plane of local geodetic horizon approximately, pointing to the east. The baseline length is approximate 1m, which is demonstrated in Fig.1. During about 800 seconds observation, the number of available satellites equals seven for GPS and eight for Compass most of the time, with a few drops to seven. The constellation of GPS satellites in this experiment is shown in Fig.2 and the constellation of Compass satellites in this experiment is shown in Fig.3, and each satellite is discernible by its PRN number. Note that the star symbol denotes the geostationary satellites of Compass.

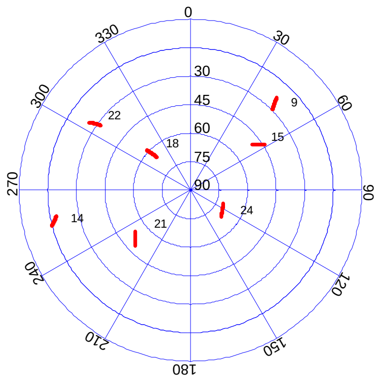

Fig.2 The constellation of GPS satellites

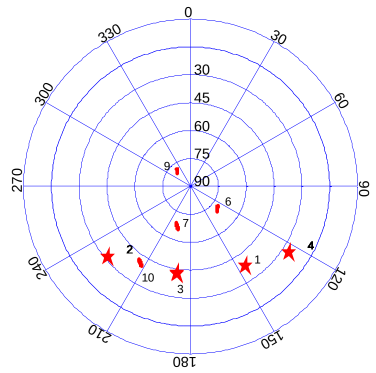

Fig.3 The constellation of Compass satellites

B. Comparison of Attitude Determination

The heading/yaw and elevation/pitch are resolved based on the model (23) with Constrained (C-) LAMBDA method.

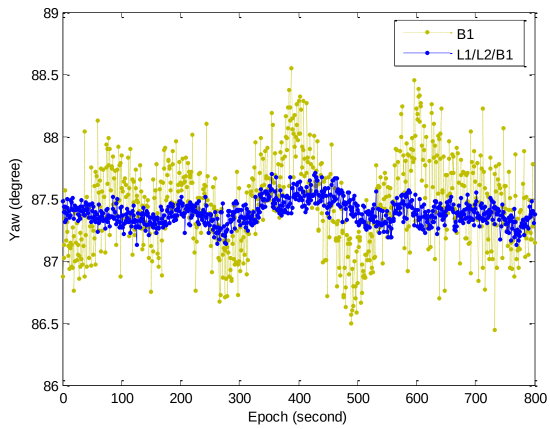

Fig.4 The yaw comparison for L1/L2/B1 and only B1 schemes

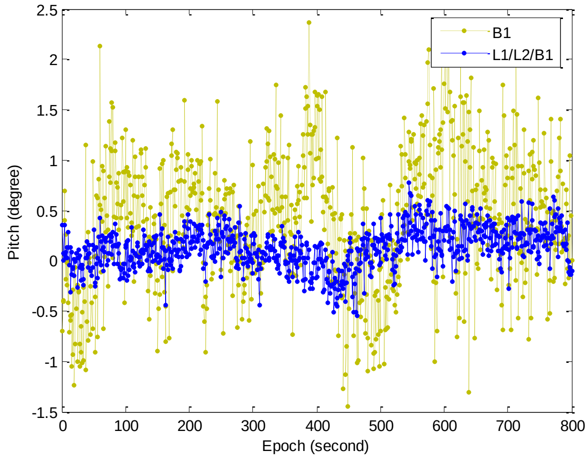

Fig.5 The pitch comparison for L1/L2/B1 and only B1 schemes

The yaw and pitch results are demonstrated in Fig.5 and Fig.6, respectively. As is shown, the accuracy of L1/L2/B1 scheme is much higher than that of the B1 scheme. The resolved baseline length is also given in Fig.6. Also, the baseline length of L1/L2/B1 scheme has a smaller noise level than that of the B1 scheme.

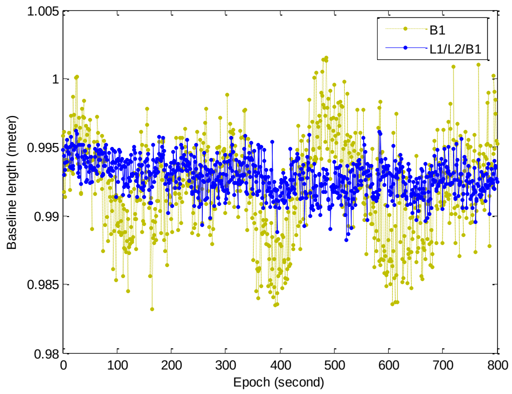

Fig.6 The baseline length comparison for L1/L2/B1 and B1 schemes

C. *Accuracy Assessment of Attitude Determination*

As shown in Table I, the average and standard deviation of attitude angle measurements of various methods are given.

TABLE I. ACCURACY ASSESSMENT FOR ONE METER BASELINE

Table Head	Mean Value (degree)		Standard deviation (degree)	
	Yaw	*Pitch*	*Yaw*	*Pitch*
B1	87.4498	0.4088	0.3609	0.6669
L1/L2	87.4555	0.0003	0.1422	0.3004
L1/L2/B1	87.3876	0.1232	0.0979	0.2015

This indicates the L1\L2\B1 can obtain the optimal accuracy compared to the other two schemes listed in the table. For the baseline with one meter length, the accuracy of yaw can reach 0.1 degree and the accuracy of elevation can reach 0.2 degree for L1/L2/B1 triple-frequency combination observation and it is two times higher than that of the single frequency observation and about 1.5 times higher than that of L1/L2 dual frequency observation. With the actual experimental results above, the correctness of proposed method for multiple constellations can be verified.

REFERENCES

[1] C.H. Tu, K.Y Tu, F.R. Chang and L.S. Wang, "GPS compass: a novel navigation equipment," IEEE Trans Aerosp Electron Sys, vol. 33, pp. 1063–1068, July 1996.

[2] A. Leick, GPS satellite surveying, 3rd ed., Wiley, New York, 2004, pp.324-337.

[3] P.J.G Teunissen, "Integer least squares theory for the GNSS Compass," Journal of Geodesy, vol. 83, pp. 1-15, January 2010.

[4] M. Shirazian, L.E. Sjoberg, M. Horemuz, "A remark on the GNSS differenced phase ambiguity parameters," Acta Geodaetica et Geophysica, vol.46, pp 431-440, Decemeber 2011.

[5] W. Chen, X. Li, "Success rate improvement of single epoch integer least-squares estimator for the GNSS attitude/short baseline applications with common clock scheme," Acta Geodaetica et Geophysica, vol.49, pp. 295-312, September 2014.

[6] P.J.G Teunissen, "The LAMBDA method for the GNSS compass," Artif. Satellites, vol. 41, pp. 89-105, July 2007.

[7] C. Park, P.J.G Teunissen, "Integer least squares with quadratic equality constraints and its application to GNSS attitude determination systems," Int J Control Autom Syst, vol.7, pp. 566-576, December 2009.

[8] P.J.G Teunissen, G. Giorgi, P.J Buist, "Testing of a new single-frequency GNSS carrier-phase compass method: land, ship and aircraft experiments," GPS Solutions, vol. 15, pp. 15-28, January 2011.

[9] W. Chen, H. Qin, Y. Zhang, T. Jin, "Accuracy assessment of single and double difference models for the single epoch GPS compass", Advances in Space Research, vol. 49, pp. 725-738, Decemeber 2012.

[10] X.W Chang, C.C Paige, "Code and carrier phase based short baseline GPS positioning: Computational aspects", GPS Solutions, vol 7, pp.230-240, October 2004.

[11] W. Chen, Y. Zhang, "Assessment of GNSS Orthogonal Transformation Model", The Jounal of Navigation, Vol. 65, pp. 561-570, July 2012.

[12] C. Hegarty, E. Powers, B. Fonville. "Accounting for timing biases between GPS, modernized GPS, and Galileo signals", Proceedings of the 36th Annual Precise Time and Time Interval (PTTI) Systems and Applications Meeting, 7-9 December 2004, Washington, D.C.